Experimental observation of the marginal glass phase in a colloidal glass

Andrew P. Hammond[a,b,1] and Eric I. Corwin[a,b]

[a]Materials Science Institute, University of Oregon, Eugene, OR 97403; and [b]Department of Physics, University of Oregon, Eugene, OR 97403

Edited by Pablo G. Debenedetti, Princeton University, Princeton, NJ, and approved February 5, 2020 (received for review October 3, 2019)

The replica theory of glasses predicts that in the infinite dimensional mean field limit, there exist two distinct glassy phases of matter: stable glass and marginal glass. We have developed a technique to experimentally probe these phases of matter using a colloidal glass. We avoid the difficulties inherent in measuring the long time behavior of glasses by instead focusing on the very short time dynamics of the ballistic to caged transition. We track a single tracer particle within a slowly densifying glass and measure the resulting mean squared displacement (MSD). By analyzing the MSD, we find that upon densification, our colloidal system moves through several states of matter. At lowest densities, it is a subdiffusive liquid. Next, it behaves as a stable glass, marked by the appearance of a plateau in the MSD whose magnitude shrinks with increasing density. However, this shrinking plateau does not shrink to zero; instead, at higher densities, the system behaves as a marginal glass, marked by logarithmic growth in the MSD toward that previous plateau value. Finally, at the highest experimental densities, the system returns to the stable glass phase. This provides direct experimental evidence for the existence of a marginal glass in three dimensions.

glass | Gardner | marginal glass | colloid

Glasses are ubiquitous, and yet a first-principles theory explaining their properties remains elusive. A snapshot of the configuration of molecules in a glass appears to be the same as that of a dense liquid, and yet glasses are solids not liquids. The recently proposed replica theory of glasses has overcome this lack of a structural signature and provides a first-principles theory (1–8). This theory predicts two distinct glass phases: a stable glass phase, characterized by an energy landscape of multiple disconnected local minima, and a marginal glass phase, characterized by an energy landscape of basins broken into subbasins, which are themselves broken into subbasins, ad infinitum. The marginal phase has been observed in multiple simulations (9–14); however, it is not known whether the replica theory is applicable to an experimental glass. Here, we show that such a phase does exist in a slowly densifying colloidal glass, providing thermal experimental confirmation of the replica theory of glasses. We use the mean squared displacement (MSD) of individual colloids at extremely short time and length scales as an assay to determine the phase of matter. By observing as a function of density, we find evidence for a reentrant marginal phase and can begin to map out the phase diagram for colloidal glasses and compare it to the mean field result (6, 14). Our results demonstrate that colloidal glasses self-organize into a hierarchy of subbasins characteristic of a marginal phase. The existence of which provides evidence for a series of thermodynamic phase transitions underlying the dramatic change in behavior seen between a liquid and a glass. This work provides a blueprint to creating a complete phase diagram for colloidal glasses, including behavior deep within the glassy phase. The techniques developed in this work explore a previously overlooked regime for glasses, that of the shortest time and length scales. Measuring behavior in this regime is a potent tool with which to explore previously inaccessible implications of the mean field theories of glasses and to probe new material properties.

Within the replica theory of glasses, the energy landscape of a stable glass is dominated by distinct local minima contained within smooth basins. A signature for this phase can be found in the MSD of individual particles. As in all thermal systems, at shortest times, particles will move ballistically. Because the basin is smooth, particles will rapidly explore their local cage, and the MSD will reach a flat plateau characterized by the size of the cage. This signature of the stable glass has been verified both computationally and experimentally (15–23).

The energy landscape of a glass in the marginal (also known as a Gardner) phase is superficially similar to that of a stable glass in that it is nonergodic and thus broken up into multiple independent basins. However, the energy basin in a marginal glass is itself further broken up into a "fractally dense" hierarchy of subbasins within subbasins (5, 6, 11, 24, 25). Resultingly, a stable glass at any instant in time will necessarily be found in a single particular subbasin with vanishingly small barriers to a set of nearby subbasins contained within a higher level of subbasin. Thus, as the system evolves, it will first efficiently explore the local subbasin until such time as it experiences a large enough fluctuation to transition into a higher-order subbasin. For longer times, it will explore this higher order subbasin, contained within a yet larger energy barrier.

As time increases, the system will explore progressively larger regions of the energy landscape that are separated from the rest by progressively larger energy barriers. Each time the system breaks out of a subbasin into a higher-order subbasin, the MSD will be characterized by growth, as the system suddenly has access to more of phase space, followed by a plateau as the system fully explores this newly accessible space. Due to the hierarchical nature of the energy landscape, the system will exhibit

Significance

Glass is one of the easiest materials to work with, capable of forming complex and sophisticated structures with relative ease in the hands of a glass blower. However, the underlying physical principles that allow glass to slowly melt and flow are among the least understood. Recent theoretical breakthroughs hope to reveal a new kind of underlying simplicity within glasses, one that might extend to all manner of disordered and complex materials. By studying the formation of a model glass system at extremely short time scales and small length scales, we have proven the central prediction of these theories, that glasses undergo an extremely subtle transition while forming, which controls their physical properties.

Author contributions: A.P.H. and E.I.C. designed research; A.P.H. performed research; A.P.H. and E.I.C. contributed new reagents/analytic tools; A.P.H. and E.I.C. analyzed data; and A.P.H. and E.I.C. wrote the paper.

The authors declare no competing interest.

This article is a PNAS Direct Submission.

[1]To whom correspondence may be addressed. Email: ahammon7@uoregon.edu.

This article contains supporting information online at https://www.pnas.org/lookup/suppl/doi:10.1073/pnas.1917283117/-/DCSupplemental.

First published March 3, 2020.

ever longer plateaus at ever greater length scales. In the thermodynamic limit, this series of discrete plateaus will merge into a continuous logarithmic growth of the MSD (7, 8).

For soft spheres (i.e., particles with noninfinite resistance to deformation), the glass phase diagram (sketched in Fig. 1) has been proposed to exhibit a reentrant stable glass phase (6, 14). The athermal jamming density controls the location of the onset of marginality in phase space and thus controls the density at which the marginal phase is first encountered, forming a so-called Gardner dome about the athermal jamming point (6, 14, 26). That the system is able to explore densities above jamming is due to the soft sphere interaction and the presence of thermal excitatory energy.

The existence of the marginal glass regime and its transition out of the stable glass regime has been extensively probed with numerical simulations. Examining hard and soft sphere systems, several of these simulations confirm the existence of the marginal glass (11), with some even including numerical MSDs with logarithmic-like scalings (9, 10, 13). However, other work using different algorithmic approaches contest this assessment, positing that the marginal phase is an avoided transition in low spatial dimensions (12, 27). Further, due to the high computational cost in numerical simulations, the transition from ballistic to logarithmic behavior in the MSD has never been observed.

Probing such a marginal phase in physical glasses is difficult, necessitating novel methods. The first experimental evidence compatible with the marginal glass phase was work done on an externally controlled pseudo-thermal two-dimensional disk system (28). That work was done by examining a direct replica signature similar to that employed in numerical simulations. Evidence for the Gardner phase was found by resetting the system to identical starting points and observing random quasithermal excitations to evolve the system's energy landscape into a hierarchy of subbasins. A second work, studying the Johari–Goldstein relaxation in sorbitol and xylitol under cooling to low temperature found an extreme broadening of the β relaxation distribution, consistent with the fractal roughening of the energy landscape predicted by the marginal phase (29).

In this work, we create a three-dimensional thermal colloidal glass and follow its behavior under densification. We use the MSD as a signature to characterize the glass phase as a function of elapsed time. We observe a clear signature of both the stable and marginal phases. We then qualitatively compare these results to the reentrant glassy phase diagram for colloids (6, 14) (Fig. 1) and find good agreement.

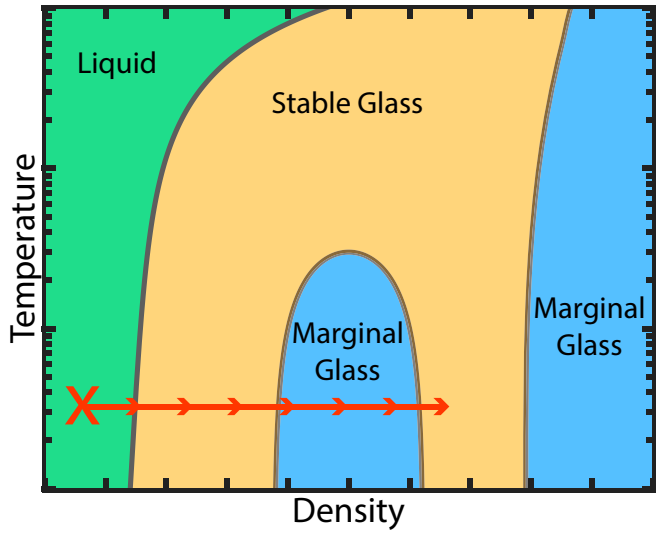

Fig. 1. Sketch of a phase diagram for soft sphere glasses as a function of temperature and density (adapted from refs. 6 and 14). Our experiment starts at the "X" and follows the arrows from the liquid to stable glass to marginal glass and then further into the stable glass phase.

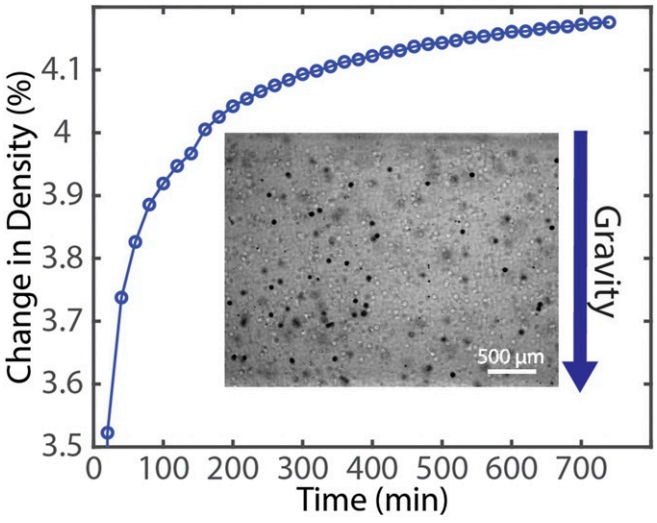

Fig. 2. Global change in density relative to the initially shaken sample versus time for a representative colloidal system. Even at the longest times studied, the system is still slowly densifying. (*Inset*) Image of the colloidal glass during sedimentation. The interstitial fluid has been index matched to the PMMA beads, so they are nearly invisible. The black tracer particles are thus revealed.

Methods

Our experimental system consists of nominally 50-μm diameter polymethyl methacrylate (PMMA) colloids (Cospheric PMPMS-1.2; 45–53 μm; $>95\%$), with 95% falling within a range of 45 to 53 μm and having sphericity of $>99\%$ and a density of 1.20 g/cm^3. The degree of polydispersity is chosen to frustrate crystallization. These colloids are suspended in a mixture of tetrahydronapthalene, decahydronapthalene, and cyclohexyl bromide. This three-component liquid is chosen to allow for precise independent control of both the refractive index and density. To this are added a small number of dyed black polyethylene tracer-colloids with the same density and diameter as the PMMA colloids (Cospheric BKPMS-1.2; 45 to 53 μm). This colloidal suspension is placed into a sealed cuvette sample chamber with an imaging width of 3 mm, large enough to allow for imaging far from any boundaries. The sealed cuvette allows us to reset the system to a new configuration by shaking it.

All imaging data were collected on a Nikon TE2000s microscope on a floating-stage optical table in a climate controlled room. Illumination is provided by a high-intensity red light-emitting diode (Thorlabs M660D2) with output of 940 mW. High-speed video was recorded on a Phantom Miro M310 high-speed camera running at 64,000 fps using an image size of 192 × 192 pixels with a total collection of 110,000 frames and a time of 1.72 s. We used a 50× lens (Nikon LU plan ELWD 50×/0.55 B, ∞/0, WD 10.1), giving us an image resolution of 0.4 μm per pixel. The cuvette being imaged is stabilized on the microscope using a custom sample holder that ensured a flat imaging plane and a minimum of vibration. The imaging stage is then encased in a small cardboard box for thermal and acoustic isolation.

We match the solutions' index to the PMMA but introduce a slight density mismatch between the fluid and the colloids causing the colloids to slowly sediment, resulting in a colloidal glass whose packing fraction increases with increasing time. We measure the average sedimentation across many samples by imaging

PHYSICS

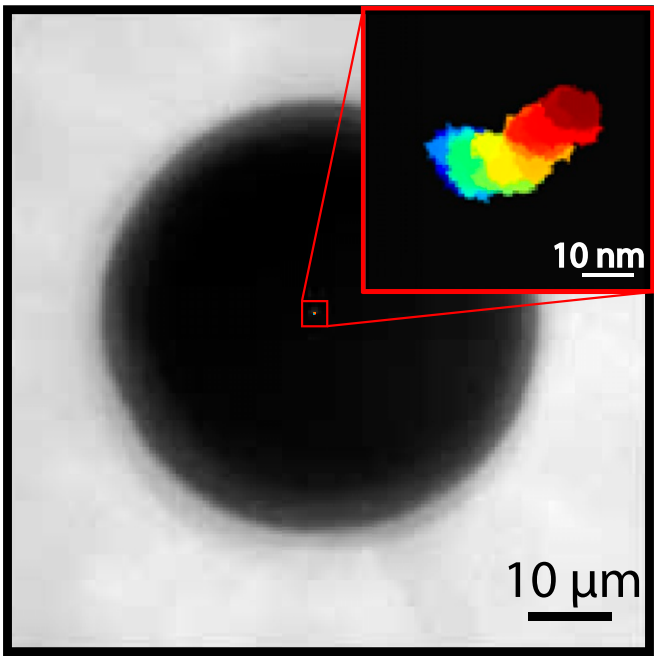

Fig. 3. Representative still image from the captured video showing the ∼50-μm diameter tracer-colloid inside the index matched colloidal glass. The tracked motion of the colloid for the entire 1.72-s video is overlayed on top of the colloid and blown up within the red box. The progression of time is represented by color running from start (blue) to end (dark red).

the whole cuvette as a function of time, as shown in Fig. 2, *Inset*. We use particle image velocimetry to analyze the flow (30) to compute the change in density versus time, a representative curve for which is shown in Fig. 2. The colloidal density always increases monotonically from the initial shaken state. The rate of densification slows over time but never stops. After the first hour, the colloids have mainly fallen out of the solution and begin to compact more slowly. The total change in packing fraction over the course of 700 min of sedimentation is about 4%.

Due to the extreme vibration sensitivity of these measurements, all data are collected late at night to ensure a minimum of human-induced noise. Before imaging, the sample cuvette is vigorously shaken from multiple directions in order to homogenize the colloidal suspension. Immediately afterward, it is placed in the cuvette holder on the microscope; at which point, a suitable tracer-colloid is selected and centered in the field of view of the camera, as shown in Fig. 3. Tracer-colloids are chosen no closer than 250 μm from the cuvette inner walls (approximately the diameter of five colloids away). Automated high-speed video of the colloid is recorded every 20 min. Over the course of the first hour, the tracer-colloid moves sufficiently that it is necessary to periodically move the stage to recenter the colloid. This motion is consistent with the large change seen in the sedimentation analysis. However, after reaching a sufficiently dense system, the tracer-colloid moves so little that the stage is locked down for all subsequent videos.

We use a radial center tracking algorithm (31) to find the center of the colloids motion in the plane perpendicular to gravity for every frame of the video, as shown in Fig. 3, *Inset*. This tracking algorithm is unbiased and has a mean localization error of ~ 1.5 nm for each frame. From these tracked data, we compute the drift-subtracted MSD for a given video as

$$\mathrm{MSD}(\tau) = \langle \|\vec{x}(t+\tau) - \vec{x}(t)\|^2 \rangle) - \|\langle \vec{x}(t+\tau) - \vec{x}(t) \rangle^2\|, \quad [1]$$

where $\vec{x}(t)$ is the measured position of the particle at time t, τ is the lag time between position measurements, and angle brackets denote a time average. Typically, the drift is an extremely small part of the MSD, affecting only the long time (i.e., $\tau > 0.1$ s) motion. Because the localization error is independent and identically distributed, we can subtract it from this MSD to achieve measurements below the nominal noise floor. This technique was employed and verified in previous work on the crossover from ballistic to diffusive motion in a freely floating colloid (32).

In order to distinguish between different forms of the MSD, we begin by finding the lag time τ^* at which the presence of other particles begins to impinge upon the motion of the tracer. We characterize this as the time when each MSD deviates by more than 10% from the Clerx–Schram expression for free floating colloidal motion (33). If the motion is logarithmic, then beyond this lag time, it should be well fit by

$$\mathrm{MSD}(\tau) = a \times \log\left(\frac{\tau}{\tau^*}\right) + x^*, \quad [2]$$

where a characterizes the slope of the logarithm, and x^* is the value of the MSD at τ^*.

Data Availability. All data discussed in the paper are available to readers upon request.

Results and Discussion

As shown in Fig. 4, we find a substantial change of behavior with increasing time and thus increasing density. The MSD of the tracer-colloid just after it has been shaken (green curves) shows ballistic motion at short times, turning over to a subdiffusive motion at long times, consistent with that of a colloid in a dense liquid suspension. At lag times of around 2×10^{-4} s, the MSD deviates from the expectation of a free floating thermal colloid (33) and instead shows subdiffusive motion (18). The absence of a diffusive regime results from the high initial colloidal density, which leads to some caging even in a freshly shaken sample. As seen in Fig. 5*A*, these MSDs are clearly not logarithmic.

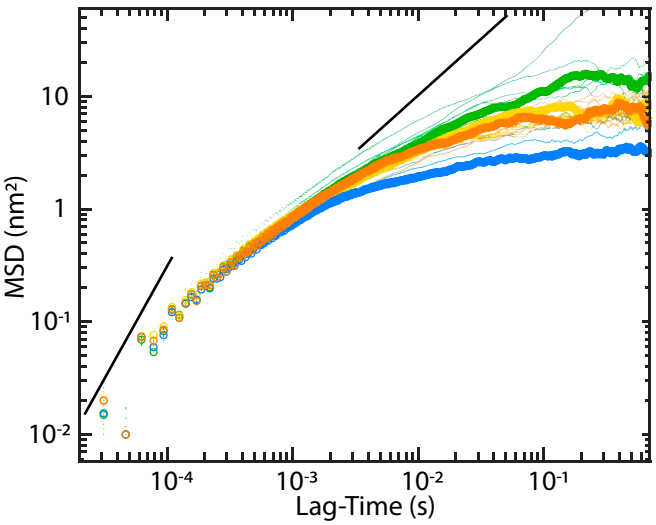

Fig. 4. MSDs from a sedimenting tracer-colloid plotted on a log-log scale. The MSDs were taken every 20 min. As a guide to the eye, we show ballistic and diffusive asymptotes demonstrating that at short times, the motion is near ballistic, and at long times, the curves are all subdiffusive. There are four important MSD regimes with a representative highlighted: from shaken to 160 min, the MSD is subdiffusive (green; 100 min); from 180 to 320 min, the MSD is plateau (yellow; 200 min); between 320 and 400 min, the MSD is logarithmic (blue; 400 min); from 420 to 520 min, the MSD is plateau, which is nearly the same as the previous plateau (orange; 580 min).

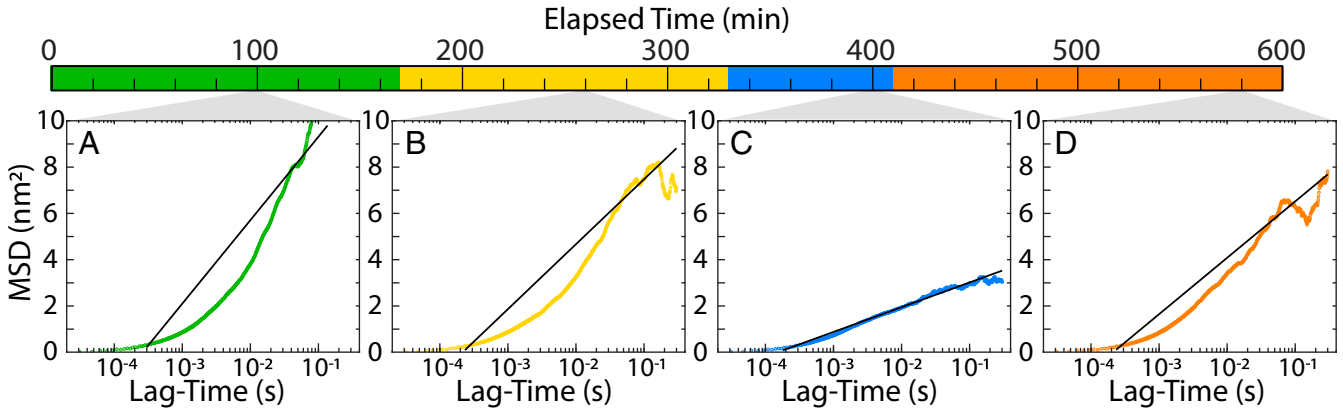

Fig. 5. Representative MSD curves from the four time steps. Superimposed on each MSD is the best fit logarithm. (*A*) MSD in the subdiffusive regime, taken at 100 min with a logarithmic fit. (*B*) MSD in the plateau regime (260 min). (*C*) MSD in the logarithmic regime (400 min). (*D*) MSD in the reentrant plateau regime (580 min).

As the colloidal density increases, the power law of the subdiffusive motion decreases toward zero. Starting at about 180 min, the MSD flattens to a plateau, indicating that the tracer-colloid is trapped inside a cage of other colloids. This behavior is shown in yellow in Fig. 4 on a log-log scale and on a semilog scale in Fig. 5*B*. This demonstrates that the system has entered into the stable glass phase. The height of the plateaus shows a small but overall consistent trend toward smaller cages, driven by the slow overall densification of the system. The transition between ballistic motion and the plateau happens slowly, over nearly three decades, only reaching the flat plateau at $\tau \sim 1 \times 10^{-1}$ s. Across all samples measured, the transition from subdiffusive to plateau happens after about 160 min.

After about 340 min, the constant plateau is replaced by an even lower MSD approaching that earlier plateau value, as shown in blue in Fig. 4. This change in the MSD is indicative of a change in phase of the underlying system. As seen in Fig. 5*C*, this motion is well fit by a logarithm. These are the only curves to demonstrate a good logarithmic fit. This behavior is indicative of the system entering the marginal glass phase. In some systems, the logarithmic MSD as a function of starting time exhibits a progression toward smaller values of the slope-fitting parameter. This implies that small changes in packing fraction result in dramatic slowing down of dynamics. Across all samples measured, the transition from plateau to logarithmic happens after about 380 min.

The system remains in the marginal phase for about 80 min (across all samples, an average of 165 min). After which, the MSDs consistently cease to be logarithmic and revert back to a constant plateau, indicating a return to the stable glass regime, shown in orange curves in Figs. 4 and 5*D*. There is no further evolution of the MSD during the experimental observation. In addition to the sedimenting tracer particle MSD shown in Figs. 4 and 5, we have included similar data for other experimental runs in *SI Appendix*.

Taken as a whole, the behavior of the densifying colloidal glass is consistent with the schematic phase diagram shown in Fig. 1. The system begins in the liquid phase, at the point marked "X." The experiment proceeds at a constant temperature but increasing density along the red line, passing through the stable glass phase, the marginal phase, and ending once again in a high-density stable glass, as shown in Fig. 5. It is striking that not only do we see individual signatures of each phase but that they combine to begin to map out a phase diagram that agrees with the theoretical predictions.

Conclusions

We have created a colloidal glass at fixed temperature and tracked it through the liquid, stable glass, and marginal glass phases as a function of increasing density. We track an individual colloid deep within the glass at short times and find the associated MSD. This experiment lays the groundwork for a complete experimental determination of the glass phase diagram by repeating such measurements over as broad a range of temperatures as possible. A full phase diagram will also allow for a careful exploration of the transition between phases to characterize what, if any, phase transitions are present in colloidal glasses. Further, the techniques developed in this work explore a previously overlooked regime for glasses, that of the shortest time and length scales. Measuring behavior in this regime is a potent tool with which to explore previously inaccessible implications of the mean field theories of glasses and to probe new material properties. The experimental observation of these distinct phases provides evidence for the validity of the replica theory of glasses in physical colloidal glasses and opens the door to an exploration of its validity in the wider world of glassy materials.

ACKNOWLEDGMENTS. We thank Dan Blair, Raghuveer Parthasarathy, and Camille Scalliet for helpful discussions and the University of Oregon machine and electrical shop staff. This work was supported by NSF Career Award DMR-1255370 and the Simons Foundation Grant 454939.

1. E. Gardner, Spin glasses with p-spin interactions. *Nucl. Phys. B* **257**, 747–765 (1985).
2. C. Brito, M. Wyart, Geometric interpretation of previtrification in hard sphere liquids. *J. Chem. Phys.* **131**, 024504 (2009).
3. G. Parisi, F. Zamponi, Mean-field theory of hard sphere glasses and jamming. *Rev. Mod. Phys.* **82**, 789–845 (2010).
4. P. Charbonneau, J. Kurchan, G. Parisi, P. Urbani, F. Zamponi, Fractal free energy landscapes in structural glasses. *Nat. Commun.* **5**, 3725 (2014).
5. S. Franz, G. Parisi, P. Urbani, F. Zamponi, Universal spectrum of normal modes in low-temperature glasses. *Proc. Natl. Acad. Sci. U.S.A.* **112**, 14539–14544 (2015).
6. G. Biroli, P. Urbani, Breakdown of elasticity in amorphous solids. *Nat. Phys.* **12**, 1130–1133 (2016).
7. P. Charbonneau, J. Kurchan, G. Parisi, P. Urbani, F. Zamponi, Glass and jamming transitions: From exact results to finite-dimensional descriptions. *Annu. Rev. Condens. Matter Phys.* **8**, 265–288 (2017).
8. L. Berthier *et al.*, Gardner physics in amorphous solids and beyond. *J. Chem. Phys.* **151**, 010901 (2019).
9. P. Charbonneau *et al.*, Numerical detection of the Gardner transition in a mean-field glass former. *Phys. Rev. E* **92**, 012316 (2015).
10. L. Berthier *et al.*, Growing timescales and lengthscales characterizing vibrations of amorphous solids. *Proc. Natl. Acad. Sci. U.S.A.* **113**, 8397–8401 (2016).
11. Y. Jin, H. Yoshino, Exploring the complex free-energy landscape of the simplest glass by rheology. *Nat. Commun.* **8**, 14935 (2017).
12. C. Hicks, M. Wheatley, M. Godfrey, M. Moore, Gardner transition in physical dimensions. *Phys. Rev. Lett.* **120**, 225501 (2018).

13. B. Seoane, F. Zamponi, Spin-glass-like aging in colloidal and granular glasses. *Soft Matter* **14**, 5222–5234 (2018).
14. C. Scalliet, L. Berthier, F. Zamponi, Marginally stable phases in mean-field structural glasses. *Phys. Rev. E* **99**, 012107 (2019).
15. P. N. Pusey, W. van Megen, Observation of a glass transition in suspensions of spherical colloidal particles. *Phys. Rev. Lett.* **59**, 2083–2086 (1987).
16. T. G. Mason, D. A. Weitz, Linear viscoelasticity of colloidal hard sphere suspensions near the glass transition. *Phys. Rev. Lett.* **75**, 2770–2773 (1995).
17. W. van Megen, T. C. Mortensen, S. R. Williams, J. Müller, Measurement of the self-intermediate scattering function of suspensions of hard spherical particles near the glass transition. *Phys. Rev. E* **58**, 6073–6085 (1998).
18. E. R. Weeks, J. C. Crocker, A. C. Levitt, A. Schofield, D. A. Weitz, Three-dimensional direct imaging of structural relaxation near the colloidal glass transition. *Science* **287**, 627–631 (2000).
19. W. K. Kegel, A. van Blaaderen, Direct observation of dynamical heterogeneities in colloidal hard-sphere suspensions. *Science* **287**, 290–293 (2000).
20. E. R. Weeks, D. A. Weitz, Subdiffusion and the cage effect studied near the colloidal glass transition. *Chem. Phys.* **284**, 361–367 (2002).
21. L. J. Kaufman, D. A. Weitz, Direct imaging of repulsive and attractive colloidal glasses. *J. Chem. Phys.* **125**, 074716 (2006).
22. G. L. Hunter, E. R. Weeks, The physics of the colloidal glass transition. *Rep. Prog. Phys.* **75**, 066501 (2012).
23. H. S. Kim, N. Şenbil, C. Zhang, F. Scheffold, T. G. Mason, Diffusing wave microrheology of highly scattering concentrated monodisperse emulsions. *Proc. Natl. Acad. Sci. U.S.A.* **116**, 7766–7771 (2019).
24. H. G. E. Hentschel, S. Karmakar, E. Lerner, I. Procaccia, Do athermal amorphous solids exist?. *Phys. Rev. E* **83**, 061101 (2011).
25. I. Procaccia, C. Rainone, C. A. B. Z. Shor, M. Singh, Breakdown of nonlinear elasticity in amorphous solids at finite temperatures. *Phys. Rev. E* **93**, 063003 (2016).
26. C. Rainone, P. Urbani, Following the evolution of glassy states under external perturbations: The full replica symmetry breaking solution. *J. Stat. Mech.* **2016**, 053302 (2016).
27. C. Scalliet, L. Berthier, F. Zamponi, Absence of marginal stability in a structural glass. *Phys. Rev. Lett.* **119**, 205501 (2017).
28. A. Seguin, O. Dauchot, Experimental evidence of the Gardner phase in a granular glass. *Phys. Rev. Lett.* **117**, 228001 (2016).
29. K. Geirhos, P. Lunkenheimer, A. Loidl, Johari-Goldstein relaxation far below T_g: Experimental evidence for the gardner transition in structural glasses?. *Phys. Rev. Lett.* **120**, 085705 (2018).
30. W. Thielicke, E. Stamhuis, PIVlab – Towards user-friendly, affordable and accurate digital particle image velocimetry in MATLAB. *J. Open Res. Software* **2**, e30 (2014).
31. R. Parthasarathy, Rapid, accurate particle tracking by calculation of radial symmetry centers. *Nat. Methods* **9**, 724–726 (2012).
32. A. P. Hammond, E. I. Corwin, Direct measurement of the ballistic motion of a freely floating colloid in Newtonian and viscoelastic fluids. *Phys. Rev. E* **96**, 042606 (2017).
33. H. J. H. Clercx, P. P. J. M. Schram, Brownian particles in shear flow and harmonic potentials: A study of long-time tails. *Phys. Rev. A* **46**, 1942–1950 (1992).